ELSEVIER

Materials Science and Engineering A226–228 (1997) 943–949

MATERIALS SCIENCE & ENGINEERING A

Dislocations and plastic deformation of quasicrystals

M. Feuerbacher [a], C. Metzmacher [a], M. Wollgarten [1,a], K. Urban [a,*], B. Baufeld [b], M. Bartsch [b], U. Messerschmidt [b]

[a] *Institut für Festkörperforschung, Forschungszentrum Jülich GmbH, D-52425 Jülich, Germany*
[b] *Max-Planck-Institut für Mikrostrukturphysik, D-06120 Halle/Saale, Germany*

Abstract

The results of experimental studies on the plastic mechanical behavior of single-quasicrystals of Al–Pd–Mn at temperatures between 680 and 800°C are reviewed. The stress–strain curves are characterized by a pronounced yield drop followed by a continuous decrease of the flow stress with increasing strain. The analysis of the microstructure of the deformed material and in-situ straining experiments in the electron microscope show that plastic deformation is based on a dislocation mechanism. The glide geometry of the dislocations can be derived from experiments in which the six-dimensional Burgers vectors and the glide planes are determined. Measurements of the thermodynamic deformation parameters, in particular, the activation volume and the activation enthalpy, indicate that dislocation motion is thermally activated and controlled by localized obstacles. These obstacles can be provided by Mackay-type clusters which form the basic structural elements according to current structure models of icosahedral Al–Pd–Mn. The decrease of the flow stress with increasing strain is explained as deformation softening caused by destruction of the structural and chemical order of the material by the motion of dislocations. © 1997 Elsevier Science S.A.

Keywords: Plastic deformation; Quasicrystals; Solid matter

1. Introduction

The quasicrystalline state of solid matter was discovered in Al–Mn alloys in 1984 [1]. For many years quasicrystal research has been dominated by efforts to clarify the nature of the structure of this novel state [2,3]. Quasilattice defects were treated theoretically [4–6] but experimental work in this field was limited. In binary alloys such as Al–Mn quasicrystalline phases occur only as metastable states and the samples are polygrained. The structure is intrinsically very defective and the grain sizes rarely reach more than a few tens of micrometers. This situation changed drastically in 1989, when new quasicrystalline phases in ternary alloy systems such as Al–Cu–Fe and Al–Cu–Co, which contain thermodynamically stable quasicrystalline phases, were discovered [7,8]. Today large single-quasicrystals of icosahedral[2] Al–Pd–Mn can be grown from the melt by the Czochralski technique [9–11]. The very high structural quality of these materials permits the investigation of defects and intrinsic physical properties. In this paper the results of plastic deformation studies of icosahedral Al–Pd–Mn single-quasicrystals are reviewed. In the course of these experiments some novel phenomena are observed, in particular, a continuous decrease of the flow stress with increasing strain.

2. Quasilattices and their six-dimensional hypercubic reference lattice

The icosahedral quasilattice is built of two different units which are a thick and a flat rhombohedron. These units are arranged in a well-defined way, according to a set of specific matching rules. In order to build a quasilattice in strict accordance with the matching rules, reference is made to a hypercubic lattice decorated with suitable hyperatoms in six-dimensional space. This hyperspace can be divided into two three-dimensional subspaces which are orthogonal to each other. One of these subspaces, the physical or parallel space, represents the real world while the second is

* Corresponding author.

[1] On leave at Department of Quantum Engineering, Nagoya University, Nagoya, Japan.

[2] Of the various types of quasicrystals only the icosahedral phases are considered here. These exhibit a structure which is quasiperiodic in all three space coordinates.

called perpendicular space. If these subspaces are suitably oriented with respect to the hypercubic lattice, the traces of the hyperatoms form a quasiperiodic arrangement of atoms in physical space, i.e. the real quasicrystal.

Strain or defects can be created in the quasilattice by displacing hyper-atoms in the six-dimensional hyperlattice from positions $\boldsymbol{X}_0$ to positions $\boldsymbol{X}_1 = \boldsymbol{X}_0 + \boldsymbol{U}$ [4]. The six-dimensional displacement vector $\boldsymbol{U}$ in general has components in physical and orthogonal space, which are called $\boldsymbol{u}_\parallel$ and $\boldsymbol{u}_\perp$ respectively. The $\boldsymbol{u}_\parallel$ components lead to translations of the atoms in physical space. As a consequence, if $\boldsymbol{U}$ is spatially variable, conventional or phonon strain is obtained in the quasilattice. The $\boldsymbol{u}_\perp$ components cause certain atoms to disappear from physical space and others to emerge in places where there were no atoms in the undisturbed quasilattice. Thus, this type of displacement leads to matching-rule violations of the corresponding quasilattice. Spatially varying $\boldsymbol{u}_\perp$ displacements resulting in matching-rule violations are called phason strain.

3. Dislocations

Dislocations are lattice defects introducing shear by highly localized atom displacements. Since defects in a quasilattice introduce both atom displacements and matching-rule violations, we have to refer to a hyperdislocation in six-dimensional reference space in order to describe a quasicrystal dislocation correctly. A dislocation can be introduced into the hyperlattice according to a generalized Volterra construction [6,12]. By removing a five-dimensional hyperlattice halfplane, a four-dimensional dislocation line is created around which displacements of the hyperatoms occur in all six space coordinates. The six-dimensional Burgers vector $\boldsymbol{B}$ of this hyperdislocation has components in physical space, $\boldsymbol{b}_\parallel$, and in orthogonal space, $\boldsymbol{b}_\perp$, according to $\boldsymbol{B} = \boldsymbol{b}_\parallel + \boldsymbol{b}_\perp$.

Two techniques allowing for the analysis of dislocations in terms of their six-dimensional Burgers vector in the transmission electron microscope have been established. The first [13] is the analogue to the classical Burgers vector analysis by Bragg diffraction contrast. For quasicrystals the conventional contrast extinction condition must be replaced by the six-dimensional relation $\boldsymbol{GB} = 0$, where $\boldsymbol{G}$ is a six-component diffraction vector. Both conventional strain and matching-rule violations are accounted for by this condition. It can be rewritten as

$$\boldsymbol{g}_\parallel \boldsymbol{b}_\parallel + \boldsymbol{g}_\perp \boldsymbol{b}_\perp = 0, \tag{1}$$

where $\boldsymbol{g}_\parallel$ and $\boldsymbol{g}_\perp$ are the components of the six-dimensional diffraction vector in physical and perpendicular space, respectively.

Two cases must be distinguished. If the first term of Eq. (1), concerning classical strain, and the second term, concerning phason strain, are non-zero but cancel each other, then the weak extinction condition is fulfilled. This case has no analogue in conventional periodic crystals. On the other hand, the terms can be individually zero. This strong extinction condition is similar to what the electron microscopist is accustomed to in normal-periodic crystals. Both conditions can be observed experimentally. This technique permits the direction of the Burgers vector of the six-dimensional reference dislocation to be determined.

Furthermore the strain-accommodation parameter, ζ, defined by

$$\zeta = \frac{|\boldsymbol{b}_\perp|}{|\boldsymbol{b}_\parallel|} \tag{2}$$

can be determined.

The experimental values [14] range from τ^3 to τ^7, where $\tau = \frac{1}{2}(1+\sqrt{5}) \approx 1.618\ldots$ is the golden mean. Thus, the phason strain component of the Burgers vector, which induces matching-rule violations, is much larger than the conventional strain component. Since matching-rule violations correspond to chemical and structural rearrangements, this means that strain in quasicrystals can effectively be accommodated by such structural changes.

The second technique [15] is based on defocused convergent-beam electron diffraction (d-CBED). The specimen is illuminated using a highly convergent electron beam giving rise to diffraction discs containing zero- or higher order Laue–Zone lines. A dislocation in the illuminated specimen area leads to a characteristic splitting of these lines. The number of splittings n is given by the generalized Cherns–Preston rule $\boldsymbol{GB} = n$. With this technique it is possible to obtain the direction and the modulus of the Burgers vector as well as the strain accommodation parameter.

4. Plastic deformation experiments on single-quasicrystals

Quasicrystals exhibit properties quite similar to those of silicon when subjected to a mechanical load at room temperature. They combine a high Vickers hardness typically between 800 and 1000 with high brittleness. Upon heating, the hardness decreases continuously and, at temperatures above about 600°C, quasicrystals become ductile. There are indications that plastic deformation at room temperature is mediated by a microcrack mechanism [16]. In the following we concentrate on high-temperature deformation between about 680 and 800°C.

For the experiments, large single-quasicrystals with the composition $Al_{70.5}Pd_{21}Mn_{8.5}$, typically about 7 cm

in length and 1 cm in diameter, were grown by the Czochralski technique. Rectangular samples of about $7 \times 2 \times 2$ mm^3 were cut with twofold planes perpendicular to the compression axis. These samples were deformed in compression in an INSTRON 8562 mechanical testing system at a constant strain rate of 10^{-5} s^{-1} [17]. In-situ tensile experiments in a high-voltage electron microscope were performed at 750°C. Experimental details are given in [18]. The microstructural investigations of deformed material were carried out in JEOL 4000FX and 2000EX electron microscopes operated at 200 kV.

5. Plastic deformation: theory

The determination of the thermodynamic activation parameters is based on the following relations [19]. The temperature dependence of the plastic strain rate $\dot{\varepsilon}_p$ is given by

$$\dot{\varepsilon}_p = \dot{\varepsilon}_0 \exp\left(-\frac{\Delta G(\tau)}{kT}\right), \tag{3}$$

where $\Delta G = \Delta H - T\Delta S$ is the activation Gibbs free energy, which in general depends on the shear stress τ. Boltzmann's constant is denoted by k, and T is the absolute temperature. ΔH is the activation enthalpy and ΔS the activation entropy. The pre-exponential factor $\dot{\varepsilon}_0$ is usually considered to be constant. Employing the thermodynamic relation

$$\left.\frac{\partial(\Delta G)}{\partial \tau}\right|_T = -V, \tag{4}$$

where V is the activation volume, one obtains from Eq. (3)

$$\left.\frac{\partial \ln \dot{\varepsilon}_p}{\partial \tau}\right|_T = \frac{V}{kT} \tag{5}$$

In stress relaxation experiments, stress is measured as a function of time after a sudden halt of the testing machine. With $\tau = m_s\sigma$, where σ is the applied stress and m_s is the Schmid factor,

$$\dot{\varepsilon} = \dot{\varepsilon}_p + C\dot{\sigma} = 0 \tag{6}$$

holds during stress relaxation, since the total strain ε is constant. C describes the elastic compliance of the specimen and the testing machine. With Eq. (5) one obtains

$$V = \frac{kT}{m_s}\left.\frac{\partial \ln(-\dot{\sigma})}{\partial \sigma}\right|_T. \tag{7}$$

Thus, the activation volume in a stress relaxation experiment can be determined from the slope of a $\ln(-\dot{\sigma})$ versus σ plot.

In the case of localized obstacles controlling the rate of plastic deformation, the activation volume is given by $V = bl\Delta x$, where b is the modulus of the Burgers vector and Δx is the distance swept by a dislocation segment of length l during thermal activation.

Differentiating Eq. (3) with respect to T yields

$$\left.\frac{\partial \ln \dot{\varepsilon}}{\partial T}\right|_T = -\left.\frac{\partial \ln \dot{\varepsilon}}{\partial \sigma}\right|_T \left.\frac{\partial \sigma}{\partial T}\right|_{\dot{\varepsilon}} = -\left.\frac{1}{kT}\frac{\partial(\Delta G)}{\partial T}\right|_\tau + \frac{\Delta G}{kT^2}$$
$$= \frac{T\Delta S + \Delta G}{kT^2} = \frac{\Delta H}{kT^2}. \tag{8}$$

Thus, the activation Gibbs free energy, which is the physically relevant parameter entering Eq. (3), is not directly accessible to experiment. However, with (5) and (8) the relation

$$\Delta H = -m_s TV \left.\frac{\partial \sigma}{\partial T}\right|_{\dot{\varepsilon}} \tag{9}$$

is obtained. Thus, the activation enthalpy can be determined by the combination of stress relaxations and temperature changes. The determination of ΔG requires additional information on the nature of the entropy terms of the activation free energy. The part of the energy which is supplied by the applied stress is the work term ΔW. Its upper bound can be calculated by $\Delta W \approx \tau V$.

6. Results of the deformation experiments

Fig. 1 shows true-stress true-strain curves at 760 and 800°C. We observe a pronounced yield drop with a maximum stress of 275 MPa. The most prominent feature is the complete absence of work-hardening. After the yield drop the stress continuously decreases with increasing strain at all temperatures. No saturation of this effect was observed up to strain values of more than 20%. Fig. 2 shows the temperature dependence of the yield stress σ_{max}. It decreases from about 750 MPa at 680°C to 120 MPa at 805°C. The activation

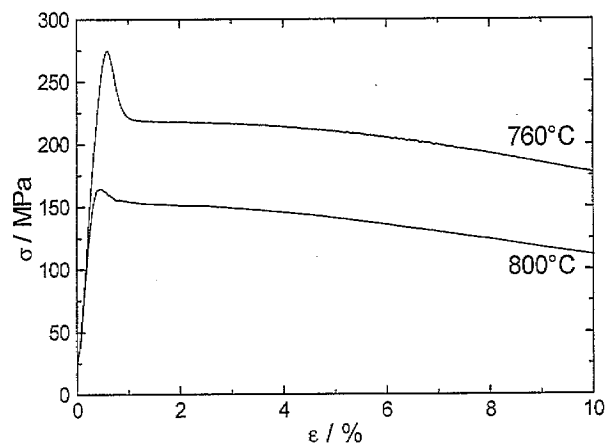

Fig. 1. Stress–strain-curves of icosahedral Al–Pd–Mn at two different temperatures (760 and 800°C) and a strain rate of 10^{-5} s^{-1}.

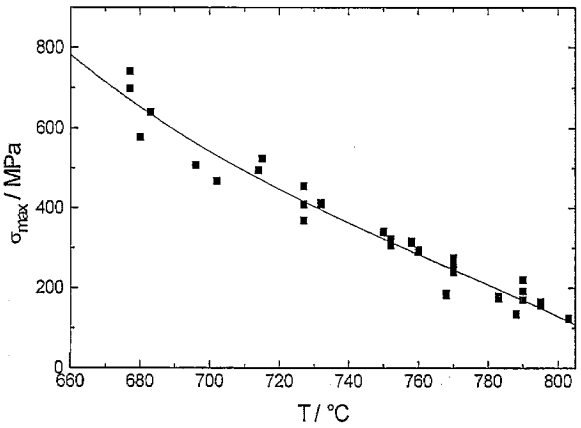

Fig. 2. Temperature dependence of the yield stress σ_{max}.

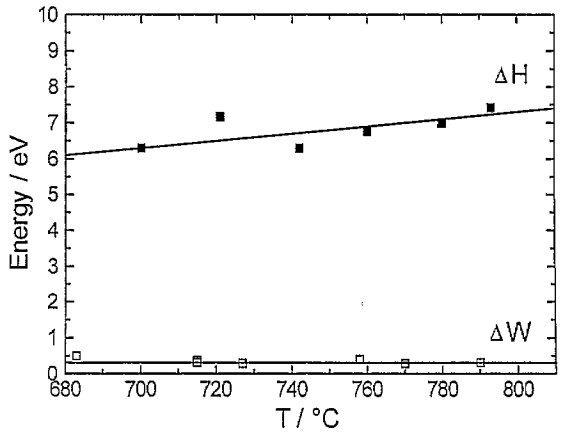

Fig. 4. Activation enthalpy ΔH and work term ΔW as a function of temperature.

volume (Fig. 3) ranges from about 1.2 nm^3 at 120 MPa to 0.16 nm^3 at 740 MPa. For the calculation of V from the experimental data according to (7), a Schmid factor $m_s = 0.5$ was inserted because of the high structural isotropy of the quasicrystal structure. The stress dependence of V can in good approximation be described by a hyperbolic function. The activation enthalpy was determined to be about 7 eV. Its temperature dependence is depicted in Fig. 4. The line is a linear fit to the data points with $\Delta H(T = 0\ \mathrm{K}) = 0$. The work term ΔW is constant in the temperature range investigated and amounts to about 0.35 eV.

7. Dislocation analysis

The dislocation density ρ as determined by electron microscopy is shown in Fig. 5 for deformation experiments carried out at 760°C as a function of plastic strain. The data points correspond to different stages of plastic deformation. The first point (0%) corresponds to an undeformed reference sample, the third (0.15%) to the upper yield point. The dislocation density increases significantly at the onset of plastic deformation. The yield drop in the stress–strain-curve (Fig. 1) is accompanied by strong dislocation multiplication. At high plastic strains, the dislocation density significantly decreases. The ratio of the dislocation density at 10% plastic strain and the maximum dislocation density amounts to 0.75. Similar behavior is observed at other deformation temperatures. However, the dislocation density decreases with increasing temperature.

More than 90% of the dislocations investigated by d-CBED in the deformed material were found to be perfect dislocations in hyperspace and showed Burgers vectors pointing along twofold quasilattice directions (in the following referred to as twofold Burgers vectors). The most frequently found Burgers vector in hyperspace is

$$A\langle 2\ \bar{1}\ \bar{1}\ 0\ 0\ 2\rangle$$

where $A = 0.645$ nm is the hyperlattice parameter [20]. This corresponds to a component in physical space of

$$\boldsymbol{b}_{\parallel} = a\langle 2/\bar{1}\ \ \bar{3}/2\ \ \bar{1}/1\rangle$$

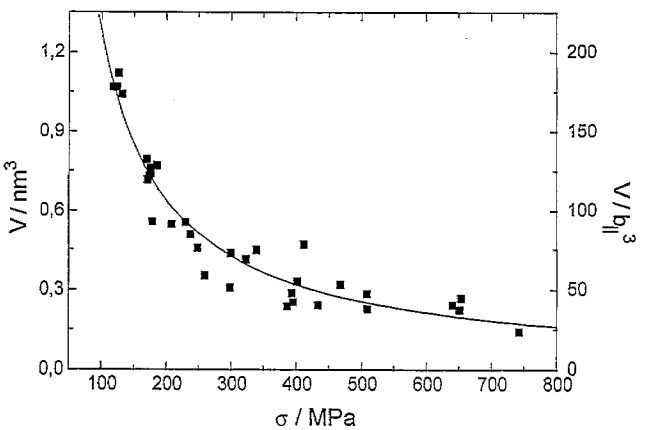

Fig. 3. Activation volume V versus stress σ. The line is a hyperbolic fit to the data points.

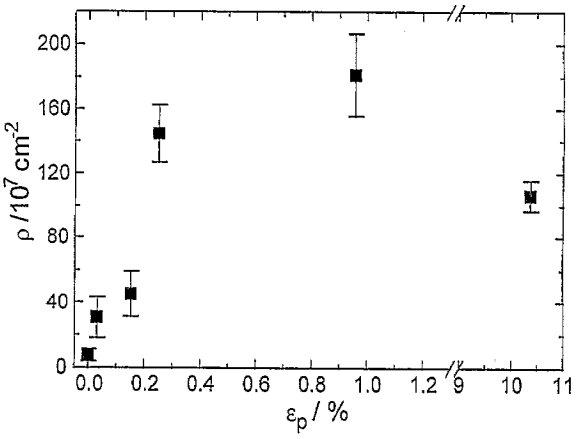

Fig. 5. Dependence of the dislocation ρ density on plastic strain at 760°C. Note the axis break.

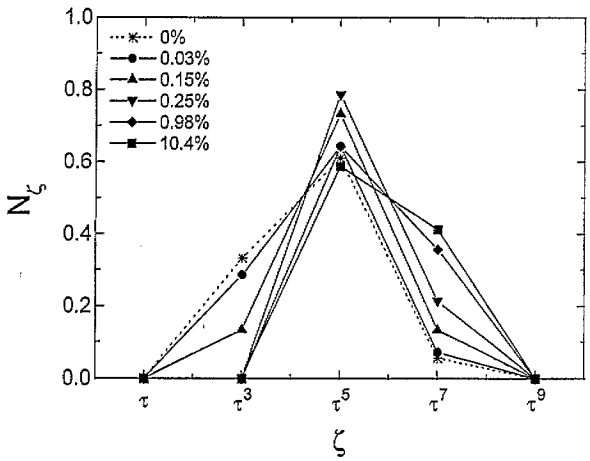

Fig. 6. Normalized ζ-distribution curves of dislocations with twofold Burgers vectors for different values of plastic strain.

in the notation of [21] where $a = 0.24$ nm. This yields a modulus of $b_\parallel = 0.183$ nm and a strain accommodation parameter of τ^5. All other dislocations, which had fivefold, threefold and pseudo-twofold Burgers vectors are partial dislocations in hyperspace. Analysis of the glide planes shows that the majority of the dislocations move on fivefold planes. Normalized distribution curves N_ζ of dislocations with twofold Burgers vectors exhibiting a given value of the strain accommodation parameter are plotted in Fig. 6 for different values of plastic strain. The curves shift to higher ζ values with increasing plastic strain.

Fig. 7 shows dislocations (black arrows) moving during an in-situ deformation experiment in a high-voltage electron microscope. The dislocation lines are slightly bowed out due to friction at the specimen surfaces. The motion is viscous, i.e. no jumps or local pinning of the dislocation line is observed. The dislocations leave behind a planar-fault contrast, which in some cases is observed to disappear after some time. The dislocations have a pronounced tendency to follow each other on the same slip trace. The planes of motion are fivefold and threefold planes. No examples of demobilization of moving dislocations by interaction processes of any kind could be observed.

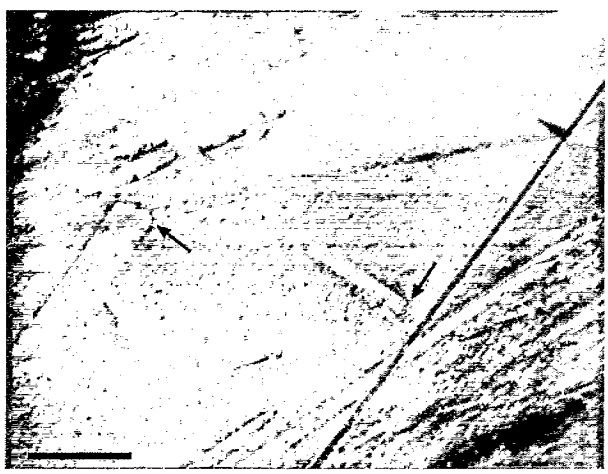

Fig. 7. Bright field image of moving dislocations during an in-situ straining experiment in a high voltage electron microscope. (Bar = 2 μm).

8. Discussion

Our results clearly indicate that plastic deformation of icosahedral quasicrystals at elevated temperatures is based on thermally activated dislocation motion. The prominent slip system consists of dislocations moving on fivefold planes with a twofold Burgers vector. Dislocation movement is controlled by localized obstacles. The observation of viscous motion in the in-situ experiments indicates that these obstacles occur at very high density so that the individual pinning and depinning processes cannot be observed in the electron microscope. On the other hand, the activation volume is about two orders of magnitude larger than the cube of the typical Burgers vector length in physical space of $b_\parallel = 0.183$ nm (Section 7). This indicates a relatively large diameter of the obstacles.

It has been argued that dislocation motion in quasicrystals, due to the creation of matching-rule violations, should be diffusion controlled [5]. However, in this case the activation volume should be of the order of the atomic volume while our experimental values are about two orders of magnitude larger. In fact, the arguments leading to diffusion control start from the assumption of an equilibrium motion of dislocations in which the static equilibrium structure of the dislocation is maintained at all times. However, our in-situ observations of dislocations leaving behind a tail of planar fault contrast can be interpreted as evidence for non-equilibrium motion of dislocations. This means that shear occurs, as a result of the applied stress, regardless of the creation of matching-rule violations. In an unlinked second step the created phason strain relaxes at a much larger timescale. This interpretation is corroborated by results of molecular dynamics simulations of shear of planar quasilattices [22]. In these, so called phason walls created by the motion of dislocations were observed which, at finite temperature, broadened considerably with time by diffusion processes.

For a further discussion we refer to the details of the structure model for Al–Pd–Mn icosahedral quasicrystals [23]. This model gives the decoration of the elementary tiles of the quasilattice with the alloy

atoms. Inspection of the atomic positions in physical space indicates that it is made up of interpenetrating clusters of icosahedral symmetry which contain 51 atoms. These so-called pseudo Mackay-clusters of about 1 nm in diameter are considered as rigid entities which are believed to be at the origin of quasicrystal phase formation and to stabilize its particular structure. In a recent study by scanning tunneling microscopy of Al–Pd–Mn surfaces produced by cleavage in ultra-high vacuum these elementary clusters could be imaged directly [24]. The fact that these clusters are hard obstacles is demonstrated by the observation that cleavage cracks avoid them, propagating instead along the mechanically softer areas between the clusters. Such behavior is also found in molecular dynamics studies of crack propagation in planar quasiperiodic lattices [25].

Assuming that Mackay-type clusters act as rate-controlling obstacles to dislocation motion, the size of the activation volume observed experimentally fits well to the value expected from the cluster size and distances as given by the structure model. This means that dislocation motion can be understood as a viscous motion through the cluster arrangement which makes up the quasilattice. Depending on the local stress situation, individual clusters are either circumvented or cut by the moving dislocations. In either case, the ordered structure of the original quasicrystal is destroyed locally by the introduction of matching-rule violations. As well known from the physics of ordered alloys, the destruction of chemical order can reduce the hardness of the material and increases its ductility. We can therefore understand the absence of any work-hardening in the stress–strain curves as the result of a deformation-induced disordering process which concerns both the chemical and the structural order and we call the observed decrease of stress with increasing strain deformation softening.

The view that the plastic behavior of single-quasicrystals is connected with the creation of phason strain, i.e. the introduction of chemical and structural disorder, is further corroborated by the high value of the activation enthalpy of about 7 eV. According to Eq. (3), the plastic strain rate is governed by the Gibbs free energy rather than the enthalpy. Finite plastic strain rates at temperatures around 750°C, for which $kT \approx 0.09$ eV, cannot be obtained without postulating a substantial deformation entropy contribution which leads to a physically reasonable value of ΔG. The disordering concept allows a part of the high activation enthalpy to be attributed to the energy increase associated with the phason strain introduced. On the other hand, the introduction of both chemical and structural disorder induces a substantial increase in the entropy of the system. These contributions are suited to arrive at a Gibbs free energy of a few electron volts in order to allow thermally activated dislocation motion at the temperature of our experiments.

9. Conclusions

Icosahedral quasilattices can be described by reference to a hypercubic lattice in six-dimensional space. Since quasilattice defects in the general case induce both conventional strain and phason strain, they likewise have to be characterized on the basis of a reference defect in hyperspace. The six-dimensional Burgers vectors of quasilattice dislocations can be analyzed by suitable contrast or diffraction experiments. Plastic deformation of quasicrystals at elevated temperatures is mediated by thermally activated motion of dislocations. Dislocation motion occurs under non-equilibrium conditions whereby a phason-strain field is left behind. The rate of plastic deformation is not controlled by diffusion but rather by localized obstacles. It is concluded that these obstacles are provided by Mackay-type clusters which are the basic elements of the Al–Pd–Mn quasicrystal structure. Dislocation motion during plastic deformation leads to the reduction of the degree of structural and chemical order. This results in deformation softening.

Acknowledgements

The authors are indebted to Professor J. Friedel and Professor J.W. Cahn for a detailed discussion at the ICQ5 Conference, Avignon, France, 1995. M. Beyss is acknowledged for the production of the single-quasicrystals.

References

[1] D. Shechtman, I. Blech, D. Gratias and J.W. Cahn, *Phys. Rev. Lett.*, *53* (1984) 1951.
[2] P.J. Steinhardt and S. Ostlund, *The Physics of Quasicrystals*, World Scientific, Singapore, 1987.
[3] C. Janot, *Quasicrystals*, Clarendon Press, Oxford, 1994.
[4] J.E.S. Socolar, T.C. Lubensky and P.J. Steinhardt, *Phys. Rev.*, *B34* (1986) 3345.
[5] T.C. Lubensky, in M.V. Jaric (ed.), *Introduction to Quasicrystals*, Academic Press, New York, 1988, p. 199.
[6] J. Bohsung and H.-R. Trebin, in M.V. Jaric (ed.), *Introduction to the Mathematics of Quasicrystals*, Academic Press, New York, 1989, p. 183.
[7] A.P. Tsai, A. Inoue and T. Masumoto, *Mater. Trans. JIM*, *30* (1989) 666.
[8] A.P. Tsai, A. Inoue, Y. Yokoyama and T. Masumoto, *Mater. Trans. JIM*, 31 (1990) 98.
[9] Y. Yokoyama, T. Miura, A.P. Tsai, A. Inoue and T. Masumoto, *Mater. Trans. JIM*, *33* (1992) 97.
[10] M. Boudard, E. Bourgeat-Lami, M. de Boissieu, C. Janot, M. Durand-Charre, H. Klein, M. Audier and B. Hennion, *Philos. Mag. Lett*, *71* (1995) 11.
[11] N. Tamura, M. Feuerbacher, M. Beyss, M. Wollgarten and K. Urban, in preparation.
[12] M. Kléman, in C. Janot and J.M. Dubois (eds.), *Quasicrystalline Materials*, World Scientific, Singapore, 1988, p. 318.

[13] M. Wollgarten, D. Gratias, Z. Zhang and K. Urban, *Philos. Mag., A64* (1991) 819.
[14] R. Rosenfeld, M. Feuerbacher, B. Baufeld, M. Bartsch, M. Wollgarten, G. Hanke, M. Beyss, U. Messerschmidt and K. Urban, *Philos. Mag. Lett., 72* (1995) 375.
[15] R. Wang and M.X. Dai, *Phys. Rev., B47* (1993) 15326.
[16] K. Urban, M. Wollgarten and R. Wittmann, *Phys. Scr., T49* (1993) 360.
[17] M. Feuerbacher, B. Baufeld, R. Rosenfeld, M. Bartsch, G. Hanke, M. Beyss, M. Wollgarten, U. Messerschmidt and K. Urban, *Philos. Mag. Lett., 71* (1995) 91.
[18] M. Wollgarten, M. Bartsch, U. Messerschmidt, M. Feuerbacher, R. Rosenfeld, M. Beyss and K. Urban, *Philos. Mag. Lett., 71* (1995) 99.
[19] U.F. Kocks, A.S. Argon and M.F. Ashby, *Thermodynamics and Kinetics of Slip*, Pergamon Press, Oxford, 1975.
[20] M. Boudard, M. de Boissieu, C. Janot, J.M. Dubois and C. Dong, *Philos. Mag. Lett., 64* (1991) 197.
[21] J.W. Cahn, D. Shechtman and D. Gratias, *J. Mater. Res., 1* (1986) 13.
[22] R. Mikulla, J. Roth and H.-R. Trebin, *Philos. Mag., B71* (1995) 981.
[23] M. Boudard, M. de Boissieu, C. Janot, G. Heger, C. Beeli, H.-U. Nissen, H. Vincent, R. Ibberson, M. Audier and J.M. Dubois, *J. Phys. Cond. Matt., 4* (1992) 10149.
[24] P. Ebert, M. Feuerbacher, N. Tamura, M. Wollgarten and K. Urban, *Phys. Rev. Lett., 77* (1996) 3827.
[25] F. Krul, R. Mikulla, P. Gumbsch and H.-R. Trebin, (submitted).